

Spatial Analogue of Quantum Spin Dynamics via Spin-Orbit Interaction

Vanita Srinivasa* and Jeremy Levy†

Department of Physics and Astronomy, University of Pittsburgh, Pittsburgh, Pennsylvania 15260, USA

We map electron spin dynamics from time to space in quantum wires with spatially uniform and oscillating Rashba spin-orbit coupling. The presence of the spin-orbit interaction introduces pseudo-Zeeman couplings of the electron spins to effective magnetic fields. We show that by periodically modulating the spin-orbit coupling along the quantum wire axis, it is possible to create the spatial analogue of spin resonance, without the need for any real magnetic fields. The mapping of time-dependent operations onto a spatial axis suggests a new mode for quantum information processing in which gate operations are encoded into the band structure of the material. We describe a realization of such materials within nanowires at the interface of LaAlO₃/SrTiO₃ heterostructures.

Quantum dynamics lies at the heart of modern physics. While the evolution of a quantum-mechanical system is governed by the time-dependent Schrödinger equation (TDSE), the mapping of this evolution from time to space has given rise to fundamental advances through the development of powerful theoretical techniques. One familiar example is provided by Feynman's path integral method [1], in which a description equivalent to the TDSE is obtained by recasting time evolution in terms of space-time paths. This approach finds applicability in a wide variety of contexts ranging from relativistic quantum mechanics to the braiding of quasiparticles that forms the basis for topological quantum computation [2]. World lines associated with quasiparticle braiding in two dimensions can be mapped to flux lines in three dimensions [3] if time itself is treated as a spatial coordinate by analytical continuation to imaginary time. In general, combining imaginary time with d spatial dimensions defines a $(d+1)$ -dimensional Euclidean space that provides a correspondence between quantum field theory and statistical mechanics [4]. Similarly, a connection between quantum field theory and quantum gravitational theory emerges through holographic mapping of a $(d+1)$ -dimensional combined space-time description to a d -dimensional one [5].

In the present work, we explore a mapping of spin dynamics from time to space, motivated by its potentially fundamental relevance to methods for coherent spin manipulation in solid-state systems [6] and physical realizations of spin-based quantum computing [7, 8]. Addressing these challenges involves harnessing the interactions of spin with spatial as well as external degrees of freedom. We show here that the coupling between spin and space can in fact be used to map the spin evolution from a temporal axis to a spatial one. Conceptually, instead of the TDSE (for $\hbar = 1$),

$$i\partial_t U(t) = H(t)U(t), \quad (1)$$

the evolution is governed by a spatial analogue, which we write as

$$i\partial_y U(y) = K(y)U(y). \quad (2)$$

The coordinate-dependent “quasimomentum operator” $K(y)$ in Eq. (2) plays a role similar to a time-varying Hamiltonian. The time-to-space mapping of spin dynamics then entails identifying a form for $K(y)$ that generates a unitary transformation $U(y)$ describing a simultaneous spatial translation and spin rotation. This identification can be made by considering the spatial analogues of time-dependent Hamiltonians $H(t)$ which generate spin dynamics.

Electron spin resonance (ESR) enables three-dimensional dynamical manipulation of single electron spins and therefore plays a central role in their promise as natural candidates for solid-state quantum bits (qubits) [9, 10]. While the Zeeman interaction describing the coupling of electron spin to external magnetic fields is typically used to carry out ESR, applying the local magnetic fields required for selectively addressing individual electron spin qubits is challenging in practice. The implementation of ESR using electric fields has therefore been widely investigated, leading to methods such as g-tensor modulation resonance (g-TMR) [11], electric dipole spin resonance (EDSR) [12–16], and ballistic spin resonance (BSR) [17].

A basic resource in both EDSR and BSR is the spin-orbit interaction, which couples the spin of an electron to its spatial motion in physical systems lacking inversion symmetry [18]. This coupling has the general form $H_{so} \propto (\vec{\nabla}V \times \vec{k}) \cdot \vec{\sigma}$ and describes the interaction of the electron spin [represented by the vector of Pauli operators $\vec{\sigma} = (\sigma_x, \sigma_y, \sigma_z)$] with an *effective* magnetic field $\vec{B}_{eff} \propto (\vec{\nabla}V \times \vec{k})$ that allows for the manipulation of spins through both an electric field \vec{E} via $\vec{\nabla}V \propto \vec{E}$ and the electronic momentum $\hbar\vec{k}$. A time-dependent oscillation of the spin-orbit interaction, generated by an external driving voltage in EDSR and internal electron dynamics in BSR, replaces the oscillating magnetic field required for ESR in these methods. The effective magnetic field due to spin-orbit coupling is also the key ingredient in several proposals for single-qubit gates [19–24].

Here, we describe a mechanism for spin resonance that relies on *spatially*-varying spin-orbit coupling and the as-

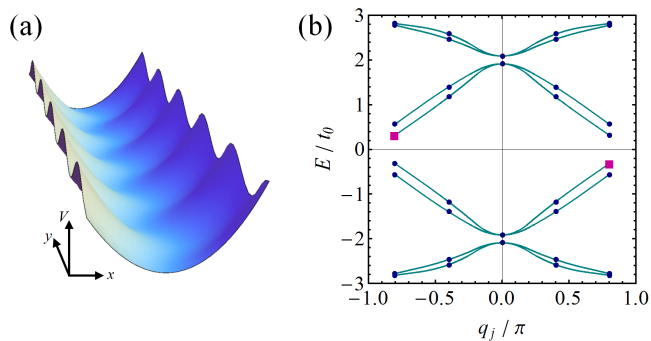


Figure 1: Spin-orbit superlattice quantum wire. (a) Schematic of a quantum wire with periodically-varying lateral confinement asymmetry which gives rise to a spin-orbit superlattice within the wire. (b) Spectrum as a function of electron quasimomentum q_j in the presence of both spatially uniform and oscillating Rashba spin-orbit coupling in perpendicular directions for $N = 20$, $m = 4$, $t_{so}^{unif}/t_0 = 1$, and $t_{so}^{osc}/t_0 = 0.125$. Filled squares indicate the eigenstates used to form the wavepacket state $|\Psi_{wp}\rangle$ discussed in the text. Lines are guides to the eye.

sociated effective magnetic field, without employing any real magnetic fields. This method maps the spin evolution from time to space and is therefore not subject to the typical time-dependent constraints imposed in quantum computing for the purpose of preserving coherence [7, 8]. We show theoretically that this “spin spatial resonance” can be achieved by creating a superlattice within a quantum wire via periodically-modulated asymmetry in the lateral confinement potential. Rather than being controlled by time-dependent external fields, spin spatial resonance is built into the spin-dependent band structure [25, 26] of the superlattice. Segments of this “designer quantum material” having fixed lengths can be used to apply spatial “pulses” that execute single-qubit gate operations on the spins of electrons which travel through the wires. Because the system is one-dimensional and gate operations are determined only by the spatial coordinate of an electron, these single-qubit gates are intrinsically “fault-tolerant” with respect to backscattering, as we discuss below.

In order to show how ESR can be mapped to space using the spin-orbit interaction alone, we first describe a “spin-orbit superlattice quantum wire,” i.e., a one-dimensional system with built-in spatially uniform [26, 27] and oscillating [25, 28, 29] spin-orbit coupling in perpendicular directions [Fig. 1(a)]. For specificity, we choose the coupling to be of the Rashba form [30], although it may be possible to realize the mapping presented here with other types of spin-orbit interaction. We assume a zero-temperature independent-electron description and represent the quantum wire confining the electronic motion to one spatial dimension using a single-band tight-binding model. In addition to a term H_0 de-

scribing the kinetic hopping of the electron along the wire, a tight-binding Hamiltonian spectrally equivalent to the Rashba spin-orbit interaction via a spin-dependent hopping can be written by discretizing the interaction on a lattice [31, 32]. We extend this tight-binding model in order to incorporate spatially-varying Rashba spin-orbit coupling. The full Hamiltonian for a wire represented by N sites with lattice constant a is given by

$$H = H_0 + H_{so}^{unif} + H_{so}^{osc}, \quad (3)$$

where

$$H_0 = -t_0 \sum_{n,\sigma} \left(c_{n+1,\sigma}^\dagger c_{n,\sigma} + \text{H.c.} \right), \quad (4)$$

$$H_{so}^{unif} = -t_{so}^{unif} \sum_{n,\sigma,\sigma'} \left[c_{n+1,\sigma'}^\dagger (i\sigma_x)_{\sigma'\sigma} c_{n,\sigma} + \text{H.c.} \right], \quad (5)$$

$$H_{so}^{osc} = -t_{so}^{osc} \sum_{n,\sigma,\sigma'} \varphi_n \left[c_{n+1,\sigma'}^\dagger (i\sigma_z)_{\sigma'\sigma} c_{n,\sigma} + \text{H.c.} \right]. \quad (6)$$

Here, the operators $c_{n,\sigma}^\dagger$ and $c_{n,\sigma}$ create and annihilate, respectively, an electron at site n with spin σ , and $t_0 = \hbar^2/2m^*a^2$, where m^* is the effective mass of the electron. The spin-dependent hopping amplitude $t_{so}^{unif} = \alpha_\perp/2a$ describes spatially uniform Rashba spin-orbit coupling of strength α_\perp generated by the potential gradient perpendicular to the plane containing the wire (defined to be the $x-y$ plane). Spatially-varying Rashba spin-orbit coupling with amplitude α_\parallel due to the potential asymmetry in the $x-y$ plane but perpendicular to the propagation direction (y axis) of the wire is incorporated via a hopping described by an amplitude $t_{so}^{osc} = \alpha_\parallel/2a$ together with a site-dependent factor φ_n . The summations in Eqs. (4)-(6) run over $n = 1, \dots, N$ and $\sigma, \sigma' = \uparrow, \downarrow$. Here, we assume periodic boundary conditions so that $n \pm N \equiv n$. Note that we choose the uniform [Eq. (5)] and oscillating [Eq. (6)] effective magnetic fields to lie along the x and z axes, respectively. In the present work, we therefore define $|\sigma\rangle \equiv |\sigma\rangle_x$; i.e., we choose the basis $\{|\uparrow\rangle_x, |\downarrow\rangle_x\}$ associated with the components of spin along the x axis in order to describe the spin orientation with respect to the effective magnetic field due to the uniform spin-orbit interaction [Eq. (5)].

In the presence of only uniform spin-orbit coupling ($t_{so}^{osc} = 0$), the energy spectrum for the Hamiltonian consists of two tight-binding bands. These bands are shifted in opposite directions along the quasimomentum axis with respect to the energy band for H_0 due to the momentum dependence of the effective magnetic field associated with the spin-orbit interaction. If the modulated Rashba spin-orbit coupling term in Eq. (6) is included in the Hamiltonian ($t_{so}^{osc} \neq 0$), the translational symmetry of the system is reduced. To map ESR spatially, we introduce periodically-varying spin-orbit coupling via

$\varphi_n = \cos(2\pi n/m)$. The Hamiltonian in Eq. (3) then retains a periodicity over m lattice sites. In this case, the energy eigenstates can be characterized by the eigenvalues of an operator D_m , which is defined to be the discrete translation operator over m sites and for which $[H, D_m] = 0$. The eigenvalues of D_m are of the form e^{iq_j} , where the associated dimensionless quasimomenta are $q_j \equiv 2\pi j/N'$, with $N' \equiv N/m$ and j an integer such that $-N'/2 \leq j < N'/2$. Letting $n = mn' + l$, we express the Hamiltonian in terms of the operators $\tilde{c}_{j,l,\sigma} \equiv \frac{1}{\sqrt{N'}} \sum_{n'=0}^{N'-1} e^{-iq_j(mn'+l)} c_{mn'+l,\sigma}$ and $\tilde{c}_{j,l,\sigma}^\dagger$. Subsequently transforming to the representation given by $d_{j,p,\sigma} \equiv \frac{1}{\sqrt{m}} \sum_{l=1}^m e^{-iQ_p l} \tilde{c}_{j,l,\sigma}$ and $d_{j,p,\sigma}^\dagger$, where $Q_p \equiv 2\pi p/m$ with p an integer such that $-m/2 \leq p < m/2$, leads to the following equivalent forms for Eqs. (4)-(6):

$$H_0 = -2t_0 \sum_{j,p,\sigma} \cos(q_j + Q_p) d_{j,p,\sigma}^\dagger d_{j,p,\sigma}, \quad (7)$$

$$H_{so}^{unif} = -2t_{so}^{unif} \sum_{j,p,\sigma} \sigma \sin(q_j + Q_p) d_{j,p,\sigma}^\dagger d_{j,p,\sigma}, \quad (8)$$

$$H_{so}^{osc} = -t_{so}^{osc} \sum_{j,p,\sigma,\sigma'} (1 - \delta_{\sigma',\sigma}) \sin\left(q_j + Q_p + \frac{\pi}{m}\right) \times \left(e^{-i\pi/m} d_{j,p+1,\sigma'}^\dagger d_{j,p,\sigma} + \text{H.c.} \right). \quad (9)$$

From the above expressions, it is evident that the kinetic hopping term H_0 and the uniform spin-orbit coupling term H_{so}^{unif} are diagonal in the basis corresponding to the operators $d_{j,p,\sigma}^\dagger$ and $d_{j,p,\sigma}$, where j indicates the quasimomentum q_j , p is a band index, and σ represents the spin component along the x axis [defined to be 1 (-1) for \uparrow (\downarrow) when used to explicitly represent the eigenvalue of σ_x , as in Eq. (8)]. The expression for H_{so}^{osc} in this basis implies that the periodically-modulated spin-orbit interaction couples “adjacent” ($\Delta p = 1$) bands having opposite spin ($\sigma' \neq \sigma$). The symmetry associated with this coupling of basis states gives rise to m -dimensional representations of the Hamiltonian. To obtain the full spectrum for Eq. (3), we numerically diagonalize the Hamiltonian matrix within each of the two m -dimensional subspaces associated with each value of q_j . As in standard ESR, we treated the oscillating effective magnetic field as a perturbation relative to the uniform effective field and choose $t_{so}^{osc}/t_0 \ll t_{so}^{unif}/t_0$. Figure 1(b) shows the spectrum as a function of q_j for $N = 20$, $m = 4$, $t_{so}^{unif}/t_0 = 1$, and $t_{so}^{osc}/t_0 = 0.125$, illustrating the coupling between the bands due to H_{so}^{osc} .

To demonstrate that signatures of spin resonance exist in the band structure of a spin-orbit superlattice quantum wire, we form a superposition of two energy eigenstates with equal and opposite quasimomenta q_j [indicated by squares in Fig. 1(b)]. Expressing these eigenstates using the notation $|j, \nu\rangle$, where $\nu = 0, 1, \dots, 7$ represents a combined spin-orbital index that is defined to increase with increasing energy E , we define

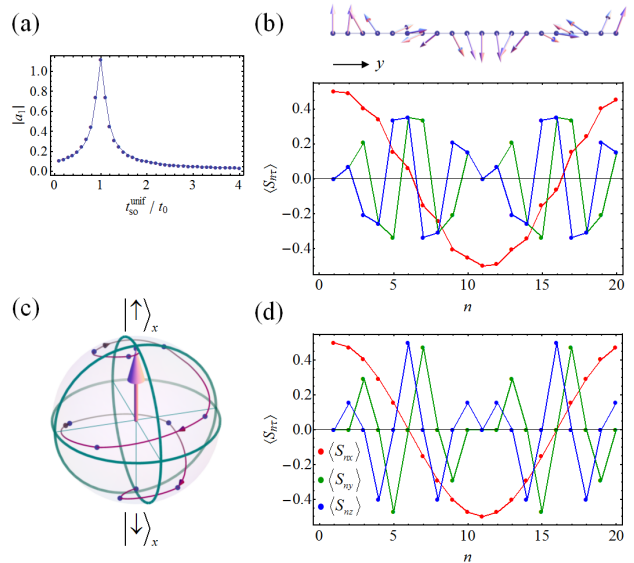


Figure 2: Spin spatial resonance. (a) Amplitude for the lowest nonzero ($l = 1$) Fourier mode of the oscillation in $\langle S_{nx} \rangle$ as a function of t_{so}^{unif}/t_0 , showing a peak at $t_{so}^{unif}/t_0 = 1$. (b) Spin polarization (in units of \hbar) for the state $|\Psi_{wp}\rangle$ at $t_{so}^{unif}/t_0 = 1$ as a function of spatial coordinate along the propagation direction (y axis) of the wire. (c) Bloch-sphere representation of the spin polarization in (b). As a function of the spatial coordinate y along the wire, the spin polarization follows a spiraling trajectory typical of spin resonance. Points indicated along the trajectory correspond to lattice sites. (d) Spin polarization components as a function of spatial coordinate for the analytical continuum model based on Eqs. (2) and (10).

a “wavepacket” $|\Psi_{wp}\rangle \equiv \frac{1}{\sqrt{2}} (|-2, 4\rangle + e^{-i\phi} |2, 3\rangle)$. Note that the variation of ϕ , which changes the relative phase between the two eigenstates, is equivalent to the time evolution of $|\Psi_{wp}\rangle$ and simply results in a shift of the phase of the oscillation in the spin polarization. We therefore fix ϕ and calculate the spin polarization as a function of site n for the wavepacket by determining the expectation values $\langle S_{n\tau} \rangle \equiv \langle \Psi_{wp} | S_{n\tau} | \Psi_{wp} \rangle$, where $S_{n\tau} \equiv |n\rangle \langle n| \otimes \frac{\hbar}{2} \sigma_\tau$ is the spin operator at site n and $\tau = x, y, z$. In the following, we let $\hbar = 1$. We use the discrete Fourier transform F_d , defined by $\langle l | F_d | n \rangle \equiv \left(1/\sqrt{N}\right) e^{-2\pi i l(n-1)/N}$, to calculate the distribution of the Fourier modes in $\langle S_{nx} \rangle$ as a function of t_{so}^{unif}/t_0 . The absolute value of the amplitude of the $l = 1$ Fourier mode, $|a_1|$ [Fig. 2(a)], has a peak for $t_{so}^{unif}/t_0 = 1$. A calculation of the spin polarization components ($\langle S_{nx} \rangle$, $\langle S_{ny} \rangle$, $\langle S_{nz} \rangle$) for the wavepacket corresponding to this peak [Fig. 2(b)] reveals that, while $\langle S_{ny} \rangle$ and $\langle S_{nz} \rangle$ vary rapidly over space, $\langle S_{nx} \rangle$ exhibits a more gradual oscillation with one full cycle over the length of the wire. The corresponding spatial dependence of the spin polarization vector is illustrated above the plot of the spin polarization components in Fig. 2(b). The Bloch-sphere evolution of the spin vector [Fig. 2(c)]

follows a spiraling path typical of ESR. Here, however, the evolution of the spin occurs with respect to a spatial coordinate - the distance along the y axis. Calculations performed for a wavepacket constructed from the two ground states $|\pm 2, 0\rangle$ reveal similar results, with a peak in $|a_1|$ at $t_{so}^{unif}/t_0 = 1$.

The above analysis based on the tight-binding model defined in Eqs. (3)-(6) is well described by an analytical model obtained from a mapping of the standard electron spin resonance formalism for a two-state system from time to space via Eq. (2). Based on the continuum version of Eq. (3), we choose the form

$$K(y) \equiv \frac{k_0}{2} \sigma_x - k_1 \cos(ky) \sigma_z \quad (10)$$

for the quasimomentum operator. Here, $k \equiv 2\pi/\lambda$ is the spatial frequency associated with oscillating spin-orbit coupling of wavelength λ . Eq. (10) has a form analogous to a spin resonance Hamiltonian, with time replaced by the spatial coordinate y along the wire and temporal frequencies replaced by their spatial counterparts. The spin polarization components can be written in terms of the matrix elements of the solution $U(y)$, which can be determined using spatial analogues of the interaction picture, the rotating wave approximation, and a transformation to a rotating frame. Choosing $\lambda = 4a$, $k_0 = (\pi/2a)(t_{so}^{unif}/t_0)$, and $k_1 = (4\pi/5a)(t_{so}^{osc}/t_0)$ in order to make a correspondence with the wavepacket state used in the tight-binding calculation described above, we let $y = na$ and evaluate the spin polarization as a function of n . The case $t_{so}^{unif}/t_0 = 1$, $t_{so}^{osc}/t_0 = 0.125$, which corresponds to the spatial resonance condition $k = k_0$ and the fundamental spatial frequency $k_1 = \pi/10a$, is shown in Fig. 2(d). This analytical result for the spin polarization components possesses qualitative features similar to the numerical result based on diagonalization of the tight-binding model for the same values of t_{so}^{unif}/t_0 and t_{so}^{osc}/t_0 [Fig. 2(b)]. The distortion of $\langle S_{nx} \rangle$ in Fig. 2(b) relative to the smooth sinusoidal variation in the continuum analytical model of Fig. 2(d) is due to the fact that the subspace of $|j, p, \sigma\rangle$ basis states for the tight-binding calculation consists of $m = 4$ rather than two states, all of which contribute to $|\Psi_{wp}\rangle$. In addition, the finite size of the system used in the tight-binding calculation results in a reduced amplitude of variation in $\langle S_{ny} \rangle$ and $\langle S_{nz} \rangle$ compared to the analytical result of Fig. 2(d). The analytically-obtained signatures of ESR are nevertheless evident in the tight-binding results for the spin-orbit superlattice quantum wire, demonstrating that it is indeed possible to achieve ESR entirely from spin-orbit coupling and map spin resonance from time to space.

We now describe a possible physical implementation of a spin-orbit superlattice quantum wire at the interface of a $\text{LaAlO}_3/\text{SrTiO}_3$ heterostructure. In this system, a local voltage-induced metal-insulator transition has been used to demonstrate both the fabrication of

nanowires with widths ~ 2 nm [33] and the incorporation of highly asymmetric potential profiles along the nanowires [34]. In principle, the same method can be used to create nanowires with built-in lateral confinement asymmetry, and periodic variation of the asymmetry of the applied pulse along the wire can give rise to spatially oscillating spin-orbit coupling. The corresponding oscillating effective magnetic field will be oriented perpendicular to the plane containing the wire (i.e., along the z axis). Together with an orthogonal effective field due to uniform spin-orbit coupling at the interface [35], this would allow for the creation of a spin-orbit superlattice quantum wire. The resonance condition $t_{so}^{unif}/t_0 = 1$ can be used to estimate the length and spatial period of the superlattice. Using the definitions of t_0 and t_{so}^{unif} , we find $a = \hbar^2/m^*\alpha_\perp$. With $\alpha_\perp = 8 \times 10^{-12}$ eV \cdot m and $m^* = 1.1m_e$, where m_e is the free electron mass, $a = 300$ nm. For $m = 4$, this corresponds to $\lambda = ma = 4a \sim 1$ μm for the oscillating spin-orbit coupling [Eq. (6)].

The spatial mapping of ESR using only spin-orbit coupling implies that single-qubit gates can also be mapped to space. These gates are built into the spin-dependent band structure of the superlattice. Because the spin polarization is determined by the distance the electron travels along the wire, segments of spin-orbit superlattice quantum wires having fixed lengths can be thought of as spatial ‘‘pulses’’ applied to an electron which traverses them. As one application of this idea, we have found that a spin-echo pulse sequence [36] can be mapped from time to space; details of this calculation will be given in a longer paper. A degree of robustness to spin qubit gate errors caused by backscattering of the electrons exists by virtue of the fact that the system is one-dimensional, so that any change in spin polarization due to backscattering can be undone if the electron again scatters into its original propagation direction.

While ESR, quantum gates, and pulse sequences are typically regarded as time-dependent processes, the mapping of these building blocks for spin manipulation onto a *spatial* axis as described in the present work suggests a new paradigm for quantum information processing. In this framework, a spin-orbit superlattice quantum wire represents a designer quantum material with a single-qubit gate encoded into its band structure. Generalization of the ideas presented here to two or more qubits would pave the way for achieving universal quantum computing via spatial encoding of quantum dynamics.

We thank J. M. Taylor, G. Burkard, and S. Smirnov for helpful discussions. This work was supported by NDSEG (V. S.), an Andrew Mellon Fellowship (V. S.), NSF (DMR-0704022) (J. L.), and ARO MURI (W911NF-08-1-0317) (J. L.).

-
- * Electronic address: vas9@pitt.edu
† Electronic address: jlevy@pitt.edu
- [1] R. P. Feynman, *Rev. Mod. Phys.* **20**, 367 (1948).
[2] C. Nayak, S. H. Simon, A. Stern, M. Freedman, and S. Das Sarma, *Rev. Mod. Phys.* **80**, 1083 (2008).
[3] D. R. Nelson, *Phys. Rev. Lett.* **60**, 1973 (1988).
[4] A. M. Tsvelik, *Quantum Field Theory in Condensed Matter Physics* (Cambridge University Press, Cambridge, 1995).
[5] L. Susskind, *J. Math. Phys.* **36**, 6377 (1995).
[6] R. Hanson and D. D. Awschalom, *Nature* **453**, 1043 (2008).
[7] D. P. DiVincenzo, *Fortschr. Phys.* **48**, 771 (2000).
[8] G. Burkard, H. A. Engel, and D. Loss, *Fortschr. Phys.* **48**, 965 (2000).
[9] D. Loss and D. P. DiVincenzo, *Phys. Rev. A* **57**, 120 (1998).
[10] R. Hanson, L. P. Kouwenhoven, J. R. Petta, S. Tarucha, and L. M. K. Vandersypen, *Rev. Mod. Phys.* **79**, 1217 (2007).
[11] Y. Kato, R. C. Myers, D. C. Driscoll, A. C. Gossard, J. Levy, and D. D. Awschalom, *Science* **299**, 1201 (2003).
[12] E. I. Rashba and A. L. Efros, *Phys. Rev. Lett.* **91**, 126405 (2003).
[13] Y. Kato, R. C. Myers, A. C. Gossard, and D. D. Awschalom, *Nature* **427**, 50 (2004).
[14] M. Duckheim and D. Loss, *Nature Phys.* **2**, 195 (2006).
[15] V. N. Golovach, M. Borhani, and D. Loss, *Phys. Rev. B* **74**, 165319 (2006).
[16] K. C. Nowack, F. H. L. Koppens, Y. V. Nazarov, and L. M. K. Vandersypen, *Science* **318**, 1430 (2007).
[17] S. M. Frolov, S. Luscher, W. Yu, Y. Ren, J. A. Folk, and W. Wegscheider, *Nature* **458**, 868 (2009).
[18] R. Winkler, *Spin-Orbit Coupling Effects in Two-Dimensional Electron and Hole Systems*, vol. 191 of *Springer Tracts in Modern Physics* (Springer, Berlin, 2003).
[19] A. E. Popescu and R. Ionicioiu, *Phys. Rev. B* **69**, 245422 (2004).
[20] D. Stepanenko and N. E. Bonesteel, *Phys. Rev. Lett.* **93**, 140501 (2004).
[21] C. Flindt, A. S. Sørensen, and K. Flensberg, *Phys. Rev. Lett.* **97**, 240501 (2006).
[22] S. J. Gong and Z. Q. Yang, *Phys. Lett. A* **367**, 369 (2007).
[23] V. N. Golovach, M. Borhani, and D. Loss, *Phys. Rev. A* **81**, 022315 (2010).
[24] S. Nadj-Perge, S. M. Frolov, E. P. A. M. Bakkers, and L. P. Kouwenhoven, *Nature* **468**, 1084 (2010).
[25] V. Y. Demikhovskii, D. V. Khomitsky, and A. A. Perov, *Low Temp. Phys.* **33**, 115 (2007).
[26] S. Smirnov, D. Bercioux, and M. Grifoni, *Europhys. Lett.* **80**, 27003 (2007).
[27] M. Governale and U. Zülicke, *Solid State Commun.* **131**, 581 (2004).
[28] X. F. Wang, *Phys. Rev. B* **69**, 035302 (2004).
[29] G. I. Japaridze, H. Johannesson, and A. Ferraz, *Phys. Rev. B* **80**, 041308 (2009).
[30] Y. A. Bychkov and E. I. Rashba, *J. Phys. C* **17**, 6039 (1984).
[31] F. Mireles and G. Kirczenow, *Phys. Rev. B* **64**, 024426 (2001).
[32] G. Metalidis, Ph.D. thesis, Martin Luther University of Halle-Wittenberg (2007).
[33] C. Cen, S. Thiel, G. Hammerl, C. W. Schneider, K. E. Andersen, C. S. Hellberg, J. Mannhart, and J. Levy, *Nature Mater.* **7**, 298 (2008).
C. Cen, S. Thiel, J. Mannhart, and J. Levy, *Science* **323**, 1026 (2009).
[34] D. F. Bogorin, C. W. Bark, H. W. Jang, C. Cen, C. M. Folkman, C. Eom, and J. Levy, *Appl. Phys. Lett.* **97**, 013102 (2010).
[35] M. Ben Shalom, M. Sachs, D. Rakhmilevitch, A. Palevski, and Y. Dagan, *Phys. Rev. Lett.* **104**, 126802 (2010).
A. D. Caviglia, M. Gabay, S. Gariglio, N. Reyren, C. Cancellieri, and J. M. Triscone, *Phys. Rev. Lett.* **104**, 126803 (2010).
[36] L. M. K. Vandersypen and I. L. Chuang, *Rev. Mod. Phys.* **76**, 1037 (2005).